Current Recording from Sensory Cilia of Olfactory Receptor Cells In Situ

I. The Neuronal Response to Cyclic Nucleotides

STEPHAN FRINGS and BERND LINDEMANN

From the Department of Physiology, Universität des Saarlandes, D-6650 Homburg/Saar, Germany

ABSTRACT   The olfactory mucosa of the frog was isolated, folded (the outer, ciliated side faced outward), and separately superfused with Ringers solution on each side. A small number of sensory cilia (one to three) were pulled into the orifice of a patch pipette and current was recorded from them. Fast bipolar current transients, indicating the generation of action potentials by the receptor cells, were transmitted to the pipette, mainly through the ciliary capacitance. Basal activity was near 1.5 spikes s^{-1}. Exposure of apical membrane areas outside of the pipette to permeant analogues of cyclic nucleotides, to forskolin, and to phosphodiesterase inhibitors resulted in a dose-dependent acceleration of spike rate of all cells investigated. Values of 10–20 s^{-1} were reached. These findings lend further support to the notion that cyclic nucleotides act as second messengers, which cause graded membrane depolarization and thereby a graded increase in spike rate. The stationary spike rate induced by forskolin was very regular, while phosphodiesterase inhibitors caused (in the same cell) an irregular pattern of bursts of spikes. The response of spike rate was phasic–tonic in the case of strong stimulation, even when elicited by inhibitors of phosphodiesterase or by analogues of cyclic nucleotides that are not broken down by the enzyme. Thus, one of the mechanisms contributing to desensitization appears to operate at the level of the nucleotide-induced ciliary conductance. However, desensitization at this level was slow and only partial, in contrast to results obtained with isolated, voltage-clamped receptor cells.

INTRODUCTION

Olfactory receptor neurons carry long protrusions at their apical membrane—the olfactory cilia—which are embedded in a layer of mucus and are thus exposed to the odorant-containing air of the nasal cavity. Current understanding of the transduction process, which mediates olfactory reception, includes the binding of odorant to a receptor protein that is coupled to ciliary adenylate cyclase through a G protein (Pace et al., 1985). Although the involvement of ciliary adenylate cyclase cannot be assumed

for the perception of all odorants (Sklar et al., 1986), it has been demonstrated that this enzyme is stimulated by a large number of compounds that also elicit an odorant response (Lowe et al., 1989). Furthermore, in olfactory receptor cells (ORCs) a cAMP- and cGMP-gated cation channel has been discovered (Nakamura and Gold, 1987). The channel should open as a consequence of rising cAMP levels when adenylate cyclase is activated, thus providing inward current to depolarize the cell. However, these results were obtained from biochemical membrane preparations or from isolated receptor cells. The latter have an impaired response to odorants and may have other impaired functions. Intracellular signal pathways of in situ ORCs, with a good response to odorants, have not previously been investigated.

Recently, a method of recording action potential–related transients from sensory cilia of olfactory receptor cells in situ was described (Frings and Lindemann, 1988, 1990b). It can be used to study the effects of chemical stimulation on receptor cells, while maintaining the integrity of the tight junctions (which often determine the distribution of transport molecules on the cellular surface) and the integrity of the surrounding sustentacular cells (which may afford the receptor cell important homeostatic functions). Cells in situ were found to be more sensitive to odorants than isolated cells (Frings and Lindemann, 1988, 1990a, b). Using this technique, we investigated the effects of cyclic nucleotides on the activity of ORCs. Concentrations of intracellular cyclic nucleotides are expected to increase when (a) membrane-permeant nucleotides are added to the superfundate, (b) the activity of adenylate cyclase is enhanced by forskolin, or (c) the degradation of cyclic nucleotides is diminished by inhibition of nucleotide phosphodiesterase. We found that permeant analogues of cAMP and cGMP, as well as forskolin and phosphodiesterase inhibitors, stimulate the spike rate of all in situ receptor cells in a phasic–tonic way. However, pronounced differences exist in the regularity of stationary spike rates induced by these agents.

METHODS

Frogs (*Rana esculenta/ridibunda*), caught in October in Jugoslavia, were kept at 4°C in tap water and used in experiments from October to April. The frogs were killed by decapitation, the skin covering the nose was removed, and the two dorsal olfactory mucosae were excised by cutting out the triangular plate of bone that supports the epithelium on each side. After transfer to Ringers, the mucosae were carefully cut from the bone plates and used immediately or stored at 4°C.

We used the technique of ciliary recording, which was recently described (Frings and Lindemann, 1990b). Briefly, the recording chamber was a standard glass microscope slide to which a flat silicon ring was affixed. The chamber volume was near 500 μl. Two needles (200 μm thick) held the tissue, which was folded around one of them such that the mucosal surface was accessible (Fig. 1 A). A capillary (i_2) was positioned near the recording electrode, directing its outflow toward the point of recording. The method (Frings and Lindemann, 1990b) was slightly changed by increasing the angle of incidence of the stimulating fluid (see inlet tube i_2 in Fig. 1 A), thereby making possible a more reliable exchange of fluid around the tip of the pipette. By gravity, i_2 constantly delivered a stream of Ringers solution, which could be switched to a test solution by electrically actuated valves. The delay due to dead space was 8–15 s, depending on flow rate. Another inlet (i_1) served to flush the mucosal side of the chamber and thus accelerate washout of stimuli. The interstitial surface of the tissue was constantly washed with oxygenated Ringers through a separate inlet capillary (i_3). Thus chemical agents applied to

the mucosal surface could not reach the interstitial side. Fluid from both sides of the tissue was removed by overflow into a suction tube (o).

Patch pipettes were pulled from borosilicate glass and fire-polished to have resistances of 25–35 MΩ when filled with Ringers. They were filled with pipette solution and positioned with a hydraulic 3-D micromanipulator. An inverted microscope with a 40× objective was used. For recording of electrical signals a patch clamp amplifier was set to voltage clamp mode (input stage feedback resistor 1 GΩ), a pipette potential of 0 mV, and a gain of 100–200 mV/pA. For on-line scope display, signals were low-pass filtered at 300 Hz.

For the extracellular recording of action potentials (spikes) from ORCs, a pipette was positioned as shown in Fig. 1. When one or more cilia were pulled into the pipette orifice by gentle suction, fast biphasic current transients of 10–20 pA were recorded at a rate of 1–2 s^{-1} in the absence of odorants (basal spike rate). Once cilia had been pulled in for a length of 150–250 μm it was difficult to blow them out again by positive pressure. This may in part be explained by the larger diameter of the proximal ciliary segment, and in part by plugging of the tip with mucus. Thus, mixing of pipette solution and mucosal solution must have been negligible during ciliary recording. However, the electrical resistance of the pipette did not increase noticeably while cilia were pulled in. Chemical stimuli were dissolved in Ringer solution and delivered to the ciliated side of the tissue as described above.

Ciliary length was estimated by pulling cilia into a pipette of large orifice, and then withdrawing the pipette until cilia fell out. This happened when the orifice was 200–300 μm from the apical border of the tissue. Mucus was carefully washed away before such measurements.

The current signal recorded from the cilia was digitized and stored on videotape. Simultaneously, it was fed through a high-pass filter to a discriminator/rate meter of our own design. This instrument produced an on-line analogue signal calibrated in events per second, which was plotted as an experimental protocol. Computer programs were written for off-line evaluation of the current signal. The signal was low-pass filtered at 2 kHz and digitized with a sample rate of 5 kHz (12 bit) for periods of 3.5 min. From one such record 128 blocks of 8,192 data points were separately filtered (high-pass) by computing the amplitude histogram for each block and subtracting the most dominant amplitude (the low-frequency component) from all points. Fast current transients in the high-frequency component were counted as events when they exceeded one of two thresholds (dashed lines in Fig. 2 *A*), which could be set graphically, aided by the amplitude histogram. Thus, one dc time course and two event time courses of action potential–related current transients of differing amplitudes were obtained from one record. Event intervals were calculated and inverse intervals (event rates) were plotted versus time. The program allowed averaging of event rates with respect to fixed times or a fixed number of events.

The composition of the Na Ringers was (in mM): 120 NaCl, 4 NaOH, 3 KCl, 1 CaCl$_2$, 2 MgCl$_2$, 10 HEPES, 5 glucose, and 5 Na pyruvate, pH 7.4. The measured osmolarity was 250 mosM. The pipette solution contained (in mM): 115 NaCl, 4 KOH, 1 CaCl$_2$, 2 MgCl$_2$, and 10 HEPES, pH 7.4. The measured osmolarity was 229 mosM. The following compounds were obtained from Sigma (Deisenhofen, Germany): 8-bromoadenosine 3':5'-cyclic monophosphate (8BrcAMP); 8-bromoguanosine 3':5'-cyclic monophosphate (8BrcGMP); 1,3,7-trimethylxanthine (caffeine); 8-(4-chlorophenylthio)-adenosine 3':5'-cyclic monophosphate (cpt-cAMP); N^6,2'-*O*-dibutyryladenosine 3':5'-cyclic monophosphate (dbcAMP); N^2,2'-*O*-dibutyrylguanosine 3':5'-cyclic monophosphate (dbcGMP); forskolin; and 3-isobutyl-1-methylxanthine (IBMX). The nucleotides and xanthines were dissolved in Ringer solution. Forskolin was dissolved in ethanol to give a stock concentration of 10 mM. This stock was added to Ringer solution to give the indicated concentrations. Ethanol alone, at a concentration of 0.1%, had no effect on spike rate.

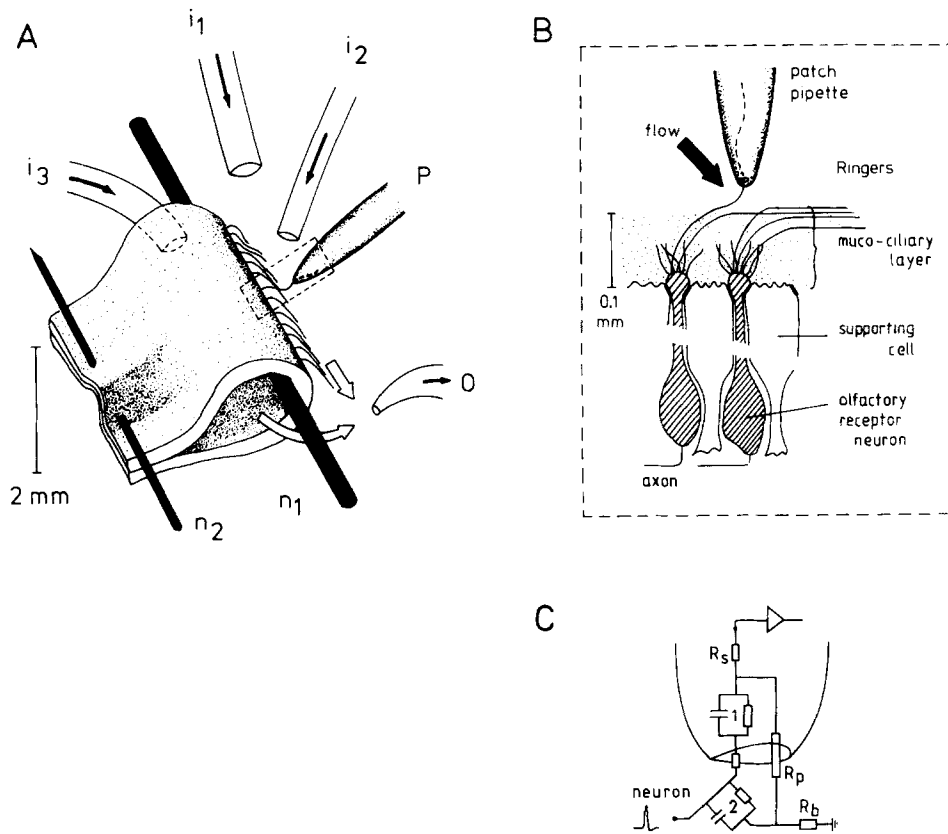Means are reported ± S.D., followed by numbers of observations (n) in brackets.

FIGURE 1. (A) Arrangement of isolated olfactory mucosa, with ciliated mucosal side facing outward, and flow system under the microscope. n_1 and n_2, needles; i_1, i_2, and i_3, inlet capillaries; o, outlet suction capillary; p, patch pipette. (B) Enlargement of boxed-in area of A, with schematical cross-section through mucosa. The muco-ciliary layer of the frog has a width of 50–100 μm when the mucosa is covered with air. In our experiments the width depended on the rate of flow of the mucosal solution. (C) Equivalent network of ciliary recording. Network 1, membrane capacitance (near 1 pF) and conductance of the part of a sensory cilium which was pulled into the patch pipette; network 2, membrane capacitance and conductance of the ciliary segment not pulled into the pipette. R_p, resistance of orifice of patch pipette (near 30 MΩ); R_s, resistance (near 1 MΩ) between electrode wire and cilium, measured after breaking a patch pipette at a point 100 μm from the tip. The electrode wire was kept at virtual ground. With R_p/R_s in the order of 30, the current transients were recorded, through the ciliary membrane acting as a capacitive electrode, with only 3–4% attenuation.

RESULTS

Recording of Transient Signals from Cilia

When the folded edge of the mounted epithelium was viewed with a 40× objective, details of the muco-ciliary layer could be distinguished. The width of this layer depended on the rate of mucosal superfusion, which tended to compress it and also

remove part of the mucus. Under normal experimental conditions the width was adjusted to values between 50 and 100 μm (Fig. 1 *B*). In the frog, the ciliary knobs of the receptor cells have short and long cilia (Hopkins, 1926; Reese, 1965). The short cilia, 20–50 μm in length, were seen to beat spontaneously in a nonsynchronized way, while the long cilia, 200–300 μm in length, did not show spontaneous movement. The long cilia were bent by the flow of mucosal solution such that their distal ends formed a dense layer oriented parallel to the mucosal surface.

A recording pipette was positioned 150–200 μm from the mucosal surface and superfusion was stopped, causing the width of the muco-ciliary layer to expand and
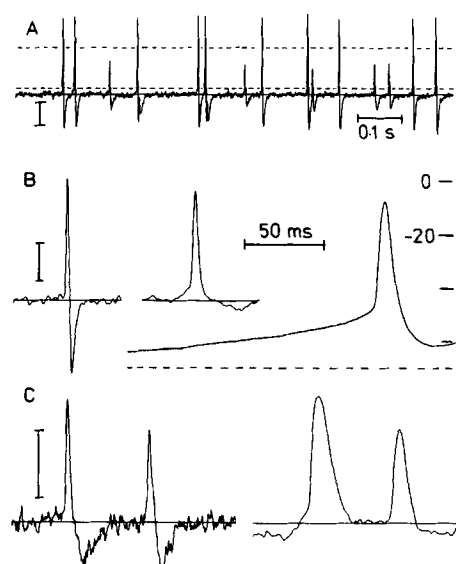
FIGURE 2. (*A*) Time sequence of biphasic current transients recorded together from cilia of two olfactory cells. The pipette was held at 0 mV and the record was low-pass filtered at 500 Hz. Record length, 1 s. The two dashed lines indicate thresholds set to discriminate transients of large and small amplitude from each other and from baseline noise. Calibration bar, 10 pA. (*B*) *Left*, typical biphasic current transient. The earlier, upward-directed halfwave represents current out of the cilium. Calibration bar, 10 pA. Numerical integration of the transient resulted in the waveform shown in the middle (vertical scale arbitrary). *Right*, action potential recorded from an ORC in situ. A gigaseal was formed with the membrane of a ciliary knob (Frings and Lindemann, 1990*a*). The whole-cell current clamp recording showed a resting potential near −70 mV (*dashed line*) and spontaneous depolarizations triggering action potentials at a rate of 0.1 s^{-1}, mostly in groups of two to four. The figure shows the first action potential of such a group. Vertical scale: membrane potential in millivolts. (*C*) Current transient recorded with 10 mM BaCl$_2$ present in the mucosal solution. Compared with *B*, the phase of capacitive inward current (second phase) was attenuated and prolonged. Calibration bar, 10 pA; time scale as in *B*. The integrated waveform, resembling an action potential of prolonged time course, is shown to the right (vertical scale arbitrary).

the long cilia to assume a more straight position. On application of gentle negative pressure to the pipette, fast biphasic transients appeared in the current signal, indicating that one or more cilia of receptor neurons firing action potentials had been pulled into the orifice. Maintaining negative pressure, the pipette was advanced to a distance of 50–100 μm from the mucosal surface, leaving a ciliary segment of at least this length exposed to the outer solution. (When the pipette was advanced further, it locally disturbed the flow of solution and therefore the regular arrangement of cilia, once superfusion was resumed.) During the advance the transients became larger, presumably because the ciliary segment shielded by the pipette

became longer. The pipette input resistance did not increase significantly above its initial value. Finally, superfusion was resumed. The success rate of this procedure was ~60%.

The current signal frequently contained transients of different amplitude, indicating that cilia from more than one neuron had been pulled into the pipette. Using threshold discrimination, transients of two amplitudes could be separated, as shown in Fig. 2 A. When more than two distinct amplitudes were recorded, only the two largest ones were separately retrieved.

Transients were usually biphasic, with the second phase having ~60% of the amplitude of the first. Fig. 2 B shows one such transient (left), as well as the result of its numerical integration (middle). If the recorded transient resulted from an action potential that was conducted into the cilium and differentiated by recording capacitive current from the ciliary membrane, then its integration should reconstruct the waveform of the action potential. This prediction was reasonably fulfilled. An

TABLE I

Mean Spike Rates of Single Units Obtained in Response to Muscosal Agents That Increase the Cellular Concentration of cAMP or cGMP

	Mucosal concentration*	Mean spike rate (n)
Basal rate	—	1.38 ± 0.58 (55)[‡]
cpt-cAMP	0.1 mM	4.91 ± 1.39 (39)[§]
8BrcGMP	0.1 mM	5.82 ± 0.87 (10)[§]
Forskolin	0.1 μM	5.61 ± 1.78 (54)[§]
IBMX	0.1 mM	5.37 ± 2.18 (30)[§]
Caffeine	3.0 mM	6.18 ± 1.42 (13)[§]

*Concentrations chosen for submaximal, steady-state responses.
[‡]Individual basal rates were obtained by averaging the instantaneous spike rate of single units over three or more minutes during mucosal superfusion with Ringers. Means ± SD from 55 such experiments.
[§]Means ± SD of n spike rates. The individual rates were obtained by averaging the instantaneous rates of single units over 20 s after onset of response.

action potential recorded from an ORC in situ in the whole-cell mode (Frings and Lindemann, 1990a) is shown in Fig. 2 B (right) for comparison.

Transients changed shape when 10 mM $BaCl_2$ was added to the mucosal solution. Essentially, the first phase remained unchanged but the second phase became prolonged and its amplitude decreased. In consequence, the integration yielded action potentials of prolonged time course (Fig. 2 C). This may be explained by the presence of Ba-blockable K channels in the apical membrane of the neurons. However, we did not find evidence for TTX-blockable Na channels in this membrane (Frings and Lindemann, 1990b; Frings et al., 1991).

In this study ciliary recording was used to test the effect of cyclic nucleotides, as putative second messengers, on the spike rate generated by olfactory receptor cells. Table I summarizes results obtained with cAMP and cGMP as well as with agents that increase the cellular concentration of cAMP.

Cyclic Nucleotides

The effects of cyclic nucleotides were investigated by superfusing the ciliary surface along the folded edge of the tissue with Ringer solution that contained membrane-permeant analogues of cAMP or cGMP. The analogues cpt-cAMP, 8BrcAMP, dbcAMP, 8BrcGMP, and dbcGMP were tested. All of these compounds increased the spike rate, but since cpt-cAMP and 8BrcGMP were found to be most potent, they were used routinely. The basal spike rate was remarkably uniform among the 225 cells investigated (1.38 ± 0.58 [55] s^{-1}). The basal rate also was quite constant during experiments, returning to its original level even after repeated strong stimulation.

All of 82 cells tested responded to cpt-cAMP with an increase of spike rate, accompanied by a decrease of spike amplitude (Fig. 3, *A* and *B*). An occasional lack of response to test solution could be corrected by reorientation of the perfusion inlet (i_2), or by removal of excessive mucus. Typically, the time course of the cpt-cAMP response was phasic–tonic, as shown in Fig. 3 *A*. When the nucleotide reached the cell, a short period of strong activity was induced, with peak rates ~15 s^{-1}. After a few seconds the rate settled at a somewhat lower plateau level which was mostly maintained until the test solution was washed out. The temporal dependence of spike rate (Fig. 3 *A*) showed a large scatter around the mean value (the solid line). Obviously, the rate was not uniform. In fact, in this experiment there was a tendency for spikes to occur in groups, with periods of ~10 s. Usually, on prolonged stimulation with cyclic nucleotides, the rate progressively stabilized (Fig. 3 *A*) and reached a stationary (plateau) level. Stationary spike sequences are shown in Fig. 3 *C*.

The plateau levels were proportional to the concentration of cpt-cAMP and were used to construct the dose–response relationships shown in Fig. 3 *D*. When the nucleotide concentration was raised above 1 mM, spike amplitudes decreased rapidly until they disappeared in the current noise. The decrease in spike amplitude was probably caused by strong and maintained membrane depolarization. Rates peaked at 20 s^{-1} as the amplitudes became unobservable. Therefore, all dose–response experiments were restricted to concentrations of 1 mM or less. When cpt-cAMP was washed out, the spike rate dropped below the basal rate (Fig. 3 *A*), often to zero. The rate returned to the basal level within 0.5–3 min, depending on the strength of the stimulus applied: the higher the rate during stimulation, the longer the depression of spike rate after washout. It is understood that the dose–effect relationships are based on extracellular concentrations and are dependent on the permeability to the nucleotide. The cellular or intraciliary concentrations of cyclic nucleotides remained unknown. When cpt-cAMP was applied to the interstitial side of the tissue for periods of 10 min, no effect on spike rate was observed.

The response to stimulation with 8BrcGMP was comparable to the cpt-cAMP effects in that the spike rate in all cells tested (24) increased to a similar extent and in a phasic–tonic manner, with an attenuated basal rate after washout. The sensitivity to 8BrcGMP was, however, somewhat higher than to cpt-cAMP. This is evident from comparing Fig. 3, *A* and *B* with Fig. 4, *A* and *B*, which show responses of the same cell stimulated with the same concentration of either nucleotide. Fig. 4 *B* shows the decrease of spike amplitude that is associated with very strong stimulation and which

probably reflects depolarization of the cell. Dose–response plots based on plateau rates (Fig. 4 C) are shown in Fig. 4 D.

Once cAMP has entered the cell through the ciliary membrane it may be expected to diffuse intracellularly into the segment shielded by the pipette. Here it should have
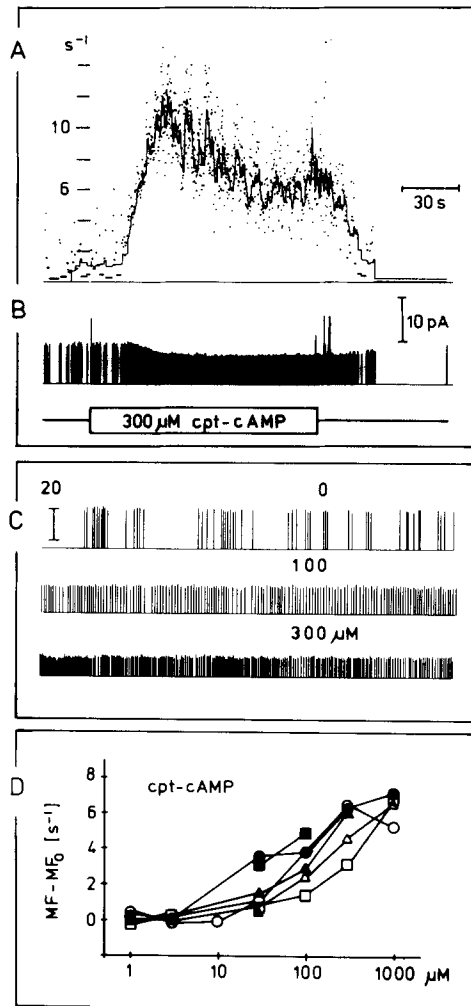

FIGURE 3. Stimulation of an ORC by application of 300 μM cpt-cAMP to the ciliary surface. The permeant nucleotide was dissolved in Ringer solution and superfused through inlet i_2 (Fig. 1 A). Electrical artifacts mark onset and end of nucleotide application. The perfusion delay was 10–15 s. (A) Plot of spike rate against time. Each point represents the inverse of the time interval between two spikes. The baseline indicates zero activity and the solid line was created by calculating the means of 10 consecutive data points. The spike rate rose from the basal value of 1.2 s^{-1} to ~11.7 s^{-1}, after which it decreased to a steady level of 6.2 s^{-1}. After washout of cpt-cAMP, the cell stopped firing until it resumed the basal rate ~2 min later (not shown). (B) Spike record from which the rate plot was generated. Note decrease of spike amplitude, which probably reflects maintained depolarization of the cell during the presence of cpt-cAMP. (C) Steady-state activity at different concentrations of cpt-cAMP. Mean rates, measured over at least 1 min, were 1.63, 5.43, and 8.17 s^{-1} at 0, 100, and 300 μM, respectively. Vertical calibration, 20 pA. Length of each trace, 30 s. (D) Steady-state dose–response relationship of mucosal cpt-cAMP (five cells). The mean basal spike rate (MF_0) was subtracted from the steady-state rate (MF) for each exposure to the nucleotide.

induced an observable inward current if cAMP-gated channels were present in the cilia. Similar "slow" currents will, of course, be generated by the apical gated channels outside the pipette, contributing to the electro-olfactogram (Persaud et al., 1988). These dc signals were easily picked up with pipettes before pulling cilia into the

orifice. Their amplitude was critically dependent on the position of the pipette, being largest when the orifice was located inside of the muco-ciliary layer. Direct currents of similar amplitude were often but not always recorded when the pipette contained cilia, and may, at least in part, have come from sources outside of the pipette. A comparison of slow currents recorded before and after aspiration of cilia was
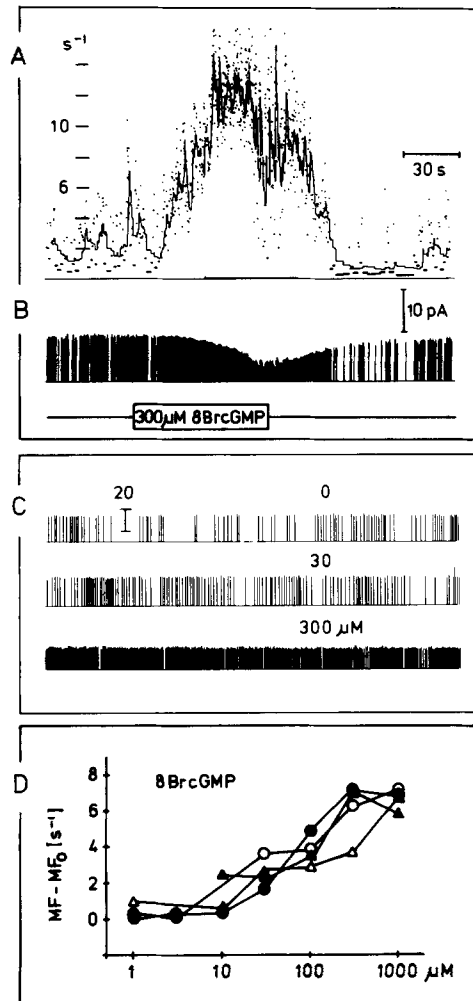

FIGURE 4. The effect of apical superfusion with 300 μM 8BrcGMP on the same cell that was shown in Fig. 3. The rate plot in *A* shows an increase of the mean spike rate from the basal value of 2 s^{-1} to a peak value of ~12.5 s^{-1}. The plateau rate was not fully established when washout began. After washout, the rate was first 0.7 s^{-1}, increasing again to 2 s^{-1} within 1 min. In *B* a progressive decrease of spike amplitude is seen. It reversed after washout. (*C*) Steady-state activity at different mucosal concentrations of 8BrcGMP. Rates were 2.37, 4.0, and 9.57 at 0, 30, and 300 μM, respectively. Vertical calibration, 20 pA. Length of each trace, 30 s. (*D*) Steady-state dose–response relationship of 8BrcGMP (four cells).

attempted. It proved difficult because the position of the pipette had to be changed in the "pulling-in" process.

Forskolin

When the ciliary surface was superfused with concentrations of forskolin >0.01 μM, the spike rate increased in a dose-dependent fashion (Fig. 5) while the spike

amplitude decreased in proportion to the spike intervals (Fig. 6 A). All of 66 cells treated with forskolin reacted in this way. If the concentration was high enough, the time course was phasic–tonic, similar to the one described above for cyclic nucleotides. The steady-state spike rate in the presence of forskolin was strikingly constant
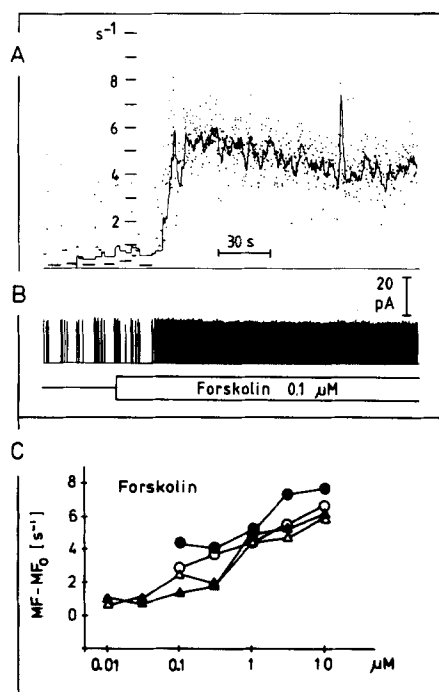

FIGURE 5. The effect of mucosal application of forskolin on the spike rate of ORCs. (A) Rate plot of the stimulation of an ORC with 0.1 μM forskolin. When forskolin was applied, the spike rate climbed from 0.5 to 5.5 s⁻¹, then decreased to a plateau level of 4.3 s⁻¹. (B) Corresponding spike record. (C) Steady-state dose–response relationships (four cells).
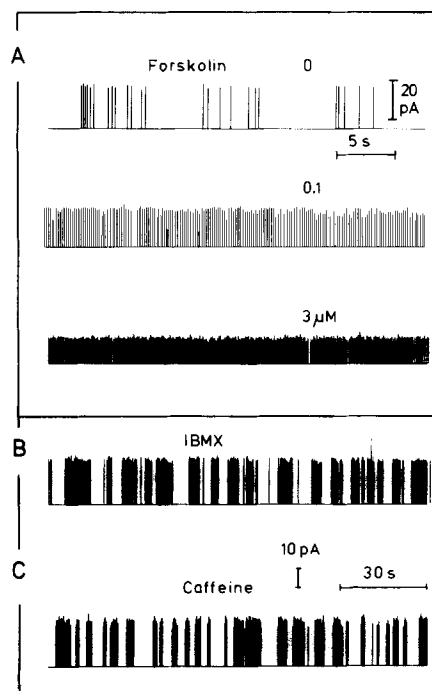
FIGURE 6. (A) Change of spike rate during superfusion of the ciliary surface with forskolin. Mean steady-state spike rates, measured over 1 min, were 0.67, 5.07, and 8.03 s⁻¹ for 0, 0.1, and 3 μM forskolin, respectively. Note the striking regularity of spike intervals and the decrease of spike amplitude with increase of spike rate. (B and C) Irregular bursting activity of two cells during prolonged stimulation with 0.3 mM IBMX (B) and 1 mM caffeine (C). The stationary bursting pattern was recorded for 8 min with IBMX and 12 min with caffeine.

(Fig. 6 A), comparable to the regular activity during the plateau phase of prolonged stimulation with cyclic nucleotides (Figs. 3 C and 4 C). In contrast, the steady-state rates were quite irregular during stimulation with phosphodiesterase inhibitors (see below and Fig. 6, B and C). Dideoxyforskolin (1 μM) had no effect.

Phosphodiesterase Inhibitors

On superfusion of the cilia with 1–100 μM IBMX (42 cells tested), a dose-dependent increase in spike rate was observed (Fig. 7, *A* and *B*). In response to a concentration step, the rate first went through a maximum, often approaching 20 s^{-1}, then decreased to a plateau rate which increased with concentration (Fig. 7 *C*). However, in contrast to the responses to cyclic nucleotides and forskolin, this level was soon interrupted by gaps in the spike activity. Thus, during prolonged exposure to IBMX, an irregular grouping of action potentials resulted (Fig. 6 *B*), distinctly different from the regular steady-state response to cyclic nucleotides or forskolin. This difference was also consistently observed when forskolin, cpt-cAMP, and IBMX were tested on the same cell. In addition, at high concentrations of IBMX (3–10 mM), spike amplitude and rate did not indicate the sustained strong depolarization of the cell, which was observed with high doses of cyclic nucleotides. Instead, strong irregular bursting behavior was observed for many minutes without a reduction of spike amplitudes. The IBMX dose–response curve (Fig. 7 *C*) showed saturation of mean spike rates above an IBMX concentration of 200 μM. The half-maximal response was seen near 40 μM. After washout of the IBMX, the spike rate was transiently decreased below the basal level, as previously observed after stimulation with cyclic nucleotides and forskolin. This phenomenon, of course, was not seen in the few cases where, as in Fig. 7, the basal rate was zero.

An irregular bursting response also occurred with prolonged application of mucosal caffeine (nine cells tested, Figs. 8, *A* and *B*, and 6 *C*). The dose–response curves show that sensitivity to caffeine was ~10 times lower than to IBMX (Figs. 7 *C* and 8 *C*), as described for other cells (e.g., Su and Hasselbach, 1984).

DISCUSSION

The Method

In the frog, an olfactory receptor cell has ~20 sensory cilia of the long variety, as well as some shorter cilia. Protruding from the apical (or sensory) knob of the dendrite, the long cilia are 200–300 μm in length and have a diameter near 0.2 μm (Hopkins, 1926; Reese, 1965). Thus, the ciliary membrane area (3,000 μm^2 or more) will exceed 90% of the soma-dendritic area of the neuron. The ciliary space constant may be on the order of 100–400 μm in the resting state (Ottoson, 1971; Trotier, D., personal communication). This value, and the "large" capacitance of 1.2 pF associated with a ciliary segment of 200 μm pulled into the pipette makes it plausible that action potentials that are conducted from soma and dendrite to the cilia will drive significant capacitive currents across the ciliary membrane. The shape of the recorded current transients (Fig. 2) supports this notion. So does the fact that the current transients disappeared when the interstitial surface of the tissue was exposed to tetrodotoxin (Frings et al., 1991).

Are the recorded transients pure capacitive currents? Voltage-gated Na currents did not seem to contribute to the signal, because application of TTX to the mucosal side had no effect (Frings et al., 1991). In contrast, when the ciliary segments not shielded by the pipette were exposed to 10 mM Ba the spike rate increased, and with

a delay transients became prolonged and their second phase attenuated (Fig. 2 C). This may be explained by Ba blocking K channels which contribute to the repolarization phase of the action potential.

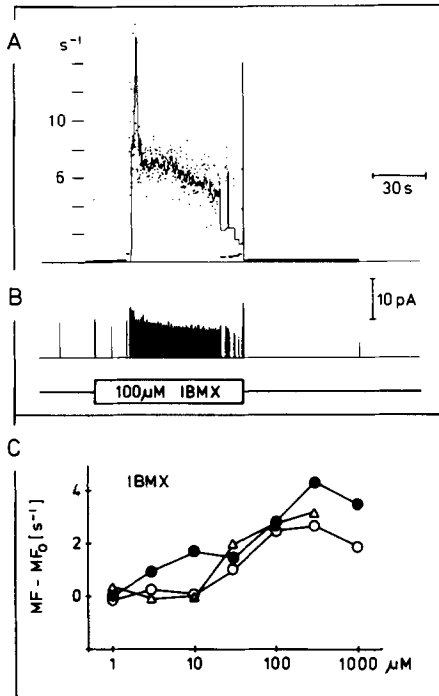Suppose the pipette contains the distal segments of two cilia from one neuron,

FIGURE 7.   The effect of mucosal application of IBMX on the spike rate of ORCs. (A and B) Rate plot and spike record of the cell of Fig. 6. When 100 μM IBMX, dissolved in Ringers, reached the cilia, the spike rate increased briefly from almost 0 to 16 s^{-1}, then declined rapidly to 6 s^{-1}. During prolonged exposures (as in Fig. 6 B) the temporal pattern changed to bursts of spikes separated by gaps, ~40 s after first response to IBMX. (C) Steady-state dose–response relationship of mucosal IBMX (three cells). Plotted are mean spike rates, averaged over bursts and gaps.
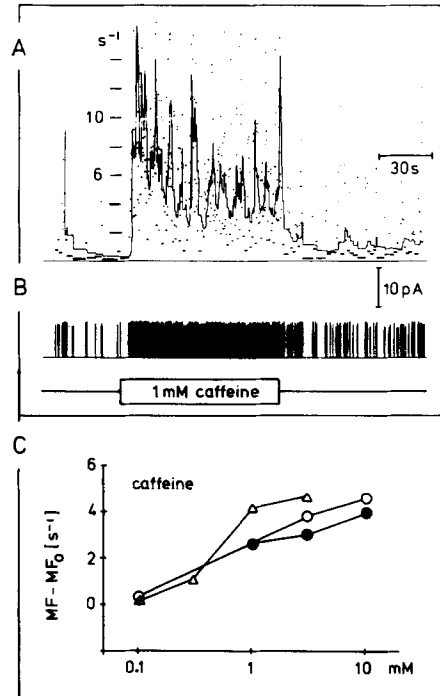
FIGURE 8.   The effect of mucosal application of 1 mM caffeine on the spike rate of ORCs. (A and B) Rate plot and spike record of a cell during superfusion of the ciliary surface with 1 mM caffeine. Note the irregular bursting activity in the spike record reflected by multiple peaks in the rate plot. (C) Stationary dose–response relationships for mucosal caffeine (three cells), indicating a 15 times lower sensitivity for this drug than for IBMX.

each for a length of 200 μm. Then 6% of the total ciliary surface is shielded by the pipette and 94% remains available for chemoreception. It is desirable to maintain the normal composition of the mucus layer while recording from the neuron. With our method, this is achieved only partially. While we are able to adjust the ion

concentrations of the superfundate, we are also increasing the mucosal volume, and normal dynamic changes of ion concentrations (Joshi et al., 1987; Trotier, D., personal communication), which may contribute to the adaptation mechanisms, will be dampened.

Furthermore, special constituents of the mucus, like the odorant-binding protein (Pevsner et al., 1988a, b; Schofield, 1988), may be washed out. We cannot exclude that this will change the odorant thresholds, but we want to point out that we did not observe changes in odorant threshold with time (Frings, S., and B. Lindemann, manuscript in preparation). Once odorant-binding protein is available in quantities, ciliary recording may be used to study its effect on odorant threshold.

When a cilium is pulled into the pipette the proximal segment of, say, 50 μm in length remains exposed to the superfundate (see equivalent network, Fig. 1 C). If this segment contains channels that open in response to odorants and second messengers, then such a response should decrease the length constant of the cilium and diminish the amplitude of the recorded current transients. A diminishment of amplitudes of the transients was regularly observed at high stimulus concentrations, accompanied by high spike rates. We are at present unable to decide whether a decrease in the ciliary space constant or a general and sustained depolarization of the neuron caused the spike amplitudes to decrease. It seems possible that the ciliary conductance is modulated by cyclic nucleotides either at the distal end of the cilia (rather than uniformly over the length of the cilium), or that this conductance is not found on the cilia but is located in other areas of the apical membrane.

The Second Messenger

Three sets of observations have implicated cAMP as a second messenger in olfactory receptor cells: (a) cAMP and phosphodiesterase inhibitors elicit transient voltage signals in the EOG that resemble the response to odorants (Minor and Sakina, 1973; Menevse et al., 1977; Persaud et al., 1988); (b) the presence in the ciliary membranes of a G protein–regulated adenylate cyclase that is activated by a variety of odorants (Pace et al., 1985; Sklar et al., 1986; Jones and Reed, 1989; Lowe et al., 1989); and (c) the demonstration in excised patches of a nonspecific cation-conducting channel of small conductance, which is present in large numbers and chemically activated by cAMP and cGMP. The channel was found in the somal membrane of isolated toad ORCs and also in membrane patches from olfactory cilia of toads (Nakamura and Gold, 1987) and catfish (Bruch and Teeter, 1989).

Our results with permeant analogues of cAMP fully support the transduction model previously proposed (e.g., Pace et al., 1985; Nakamura and Gold, 1987; Lowe et al., 1989). When applied from the mucosal side to odorant-competent ORCs in situ, the nucleotides caused a reversible increase in spike rate. The nucleotides, after entering the cilia, probably induced opening of the "Nakamura–Gold" channels (located either in the ciliary membrane or in the membrane of the apical knobs). Because of the resulting inward current, a depolarization will spread to the somal membrane and the axon hillock, causing an increase in spike rate. We also characterized the apical, cAMP-dependent conductance in terms of ion specificity. These results are described in a separate communication (Frings et al., 1991).

The difficulties encountered in recording cAMP-induced increases in inward current from the long cilia were surprising. Nakamura and Gold reported direct

currents of 10 pA generated by excised patches of ~ 0.2 μm^2 area under normal ionic conditions and membrane potentials of −60 mV (Nakamura and Gold, 1987, their Fig. 2 B). Ciliary segments 200 μm in length have areas larger than 100 μm^2. Their cAMP-induced currents should have been easily observable. This problem is presently under investigation.

Temporal Pattern and Desensitization

A reversible increase in spike rate was observed when the mucosal surface was exposed to cyclic nucleotides, but also when it was exposed to forskolin or to methylxanthines. This is expected since forskolin stimulates the adenylate cyclase, while the xanthines block cAMP breakdown by blocking the phosphodiesterase. Thus, both agents will increase the cytosolic cAMP concentration. However, the responses to these compounds differed in the temporal pattern of the resulting spike discharge. Cyclic nucleotides and forskolin induced a strikingly regular steady-state discharge, while the discharge induced by xanthines may be described as "irregular bursting."

The regular spike pattern observed in the presence of cpt-cAMP, 8BrcGMP, and forskolin may be indicative of a cellular mechanism generating oscillations of membrane potential. At low concentrations of these agents such oscillations may elicit a single action potential during each cycle when the depolarization exceeds a threshold potential. In spike trains thus generated, individual spikes are separated by the characteristic period of the oscillation (see middle traces of Figs. 3 C, 4 C, and 6 C). Both the amplitude and frequency of stimulus-dependent potential oscillations can change with stimulus strength, as has been shown for the cold receptor (Braun et al., 1980; Schäfer et al., 1988). At higher concentrations more than one action potential is elicited per cycle, resulting in the appearance of spike groups (see lower traces of Figs. 3 C, 4 C, and 6 C). As also reported by Revial et al. (1978), strong stimulation with odorants occasionally caused rhythmical bursting of the in situ ORCs (Frings and Lindemann, 1990a). Isolated ORCs frequently showed this phenomenon in response to odorants (Frings and Lindemann, 1988). Given a continuous depolarizing inward current, voltage-activated Ca channels and Ca-activated K channels may be instrumental in the generation of the oscillations (see Schäfer et al., 1986). Cellular oscillators of this type were found in a large variety of cells (Berridge and Rapp, 1979; Rapp, 1979).

The gaps in spike rate observed with the xanthines may be related to an additional effect of these compounds. In many systems caffeine is known to cause release of Ca ions from intracellular stores. This could bring about the interruptions of spike activity by activation of Ca-dependent K channels and, hence, hyperpolarization of the cell. In addition, cellular Ca may inhibit adenylate cyclase, thus decreasing the cAMP concentration (Anholt et al., 1989).

Alternatively, in view of the chemical similarities between cyclic nucleotides and xanthines, it is conceivable that xanthines compete directly with cAMP for a binding site on the "Nakamura–Gold" channel. For instance, in brain homogenates xanthines are competitors of cAMP at the cAMP binding site of the phospodiesterase (Cheung, 1967). Competitive inhibition by xanthines at the channel, together with Ca inflow

through the channels and inhibition of the cyclase by Ca, may cause the irregular bursting pattern observed. These possibilities are currently being examined.

During exposure to one of the chemical stimuli (cAMP, forskolin, or IBMX) the spike rate first increased and then declined to a smaller steady-state value (phasic–tonic response). This "adaptation" or "desensitization" was slower and not as extensive as seen with odorants in the same preparation (Frings and Lindemann 1990a,b). Since it was also observed with IBMX, it was not due to stimulation of a phosphodiesterase but to inhibition of the nucleotide-induced conductance. It appears, therefore, that adaptation consists of several steps, one of which modulates the activity of the nucleotide-induced apical conductance (see also Frings et al., 1991).

Note added in proof: Recently it was shown that, in addition to cyclic nucleotides, inositoltrisphosphate is a second messenger in olfaction (Boekhoff et al., 1990; Restrepo et al., 1990). Are the two second messenger pathways used by the same receptor cells? We like to emphasize that all receptor cells tested in our study responded to cyclic nucleotides, forskolin, and IBMX.

REFERENCES

Anholt, R. R. H., R. W. Farmer, and C. A. Karavanich. 1989. Excitation by odorants of olfactory receptor cells: molecular interactions at the ciliary membrane. *In* Chemical Senses. Vol. 1. Receptor Events and Transduction in Taste and Olfaction. J. G. Brand, R. H. Cagan, J. H. Teeter, and M. R. Kare, editors. Marcel Dekker, New York. 347–361.

Berridge, M. J., and P. E. Rapp. 1979. A comparative survey of the function, mechanism and control of cellular oscillators. *Journal of Experimental Biology.* 81:217–279.

Boekhoff, I., E. Tareilus, J. Strotmann, and H. Breer. 1990. Rapid activation of alternative second messenger pathways in olfactory cilia from rats by different odorants. *EMBO Journal.* 9:2453–2458.

Braun, H. A., H. Bade, and H. Hensel. 1980. Static and dynamic discharge patterns of bursting cold fibres related to hypothetical receptor mechanisms. *Pflügers Archiv.* 386:1–9.

Bruch, R. C., and J. H. Teeter. 1989. Second-messenger signalling mechanisms in olfaction. *In* Chemical Senses. Vol. 1. Receptor Events and Transduction in Taste and Olfaction. J. G. Brand, R. H. Cagan, J. H. Teeter, and M. R. Kare, editors. Marcel Dekker, New York. 283–298.

Cheung, W. Y. 1967. Properties of cyclic 3',5'-nucleotide phosphodiesterase from rat brain. *Biochemistry.* 6:1079–1087.

Frings, S., S. Benz, and B. Lindemann. 1991. Current recording from sensory cilia of olfactory receptor cells in situ. II. Role of mucosal Na^+, K^+ and Ca^{++} ions. *Journal of General Physiology.* In press.

Frings, S., and B. Lindemann. 1988. Odorant response of isolated olfactory receptor cells is blocked by amiloride. *Journal of Membrane Biology.* 105:233–243.

Frings, S., and B. Lindemann. 1990a. Response of olfactory receptor cells, isolated and *in situ,* to low concentrations of odorants. *In* Chemosensory Information Processing. D. Schild, editor. Springer-Verlag, Berlin. 1–8.

Frings, S., and B. Lindemann. 1990b. Single unit recording from olfactory cilia. *Biophysical Journal.* 57:1091–1094.

Hopkins, A. E. 1926. The olfactory receptors in vertebrates. *Journal of Comparative Neurology.* 41:252–289.

Jones, D. T., and R. R. Reed. 1989. G_{olf}: an olfactory neuron specific G-protein involved in odorant signal transduction. *Science.* 244:790–795.

Joshi, H., M. L. Getchell, B. Zielinski, and T. V. Getchell. 1987. Spectrophotometric determination of cation concentrations in olfactory mucus. *Neuroscience Letters.* 82:321–326.

Lowe, G., T. Nakamura, and G. H. Gold. 1989. Adenylate cyclase mediates olfactory transduction for a wide variety of odorants. *Proceedings of the National Academy of Sciences, USA.* 86:5641–5645.

Menevse, A., G. Dodd, and T. M. Poynder. 1977. Evidence for the specific involvement of cyclic AMP in the olfactory transduction mechanism. *Biochemical and Biophysical Research Communications.* 77:671–677.

Minor, A. V., and N. L. Sakina. 1973. Role of cyclic adenosine-3',5'-monophosphate in olfactory reception. *Neirofiziologiya.* 5:415–422.

Nakamura, T., and G. H. Gold. 1987. A cyclic nucleotide-gated conductance in olfactory receptor cilia. *Nature.* 325:442–444.

Ottoson, D. 1971. The electro-olfactogram. *In* Handbook of Sensory Physiology. Vol. IV. Olfaction. L. M. Beidler, editor. Springer-Verlag, Berlin. 95–131.

Pace, U., E. Hanski, Y. Salomon, and D. Lancet. 1985. Odorant-sensitive adenylate cyclase may mediate olfactory reception. *Nature.* 316:255–258.

Persaud, K. C., G. L. Heck, S. K. DeSimone, T. V. Getchell, and J. A. DeSimone. 1988. Ion transport across the frog olfactory mucosa: the action of cyclic nucleotides on the basal and odorant-stimulated states. *Biochimica et Biophysica Acta.* 944:49–62.

Pevsner, J., P. M. Hwang, P. B. Sklar, J. C. Venable, and S. H. Snyder. 1988a. Odorant-binding protein and its mRNA are localized to nasal gland implying a carrier function. *Proceedings of the National Academy of Sciences, USA.* 85:2383–2387.

Pevsner, J., R. R. Reed, P. G. Feinstein, and S. H. Snyder. 1988b. Molecular cloning of odorant-binding protein: member of a ligand carrier family. *Science.* 241:336–339.

Rapp, P. E. 1979. An atlas of cellular oscillators. *Journal of Experimental Biology.* 81:281–306.

Reese, T. S. 1965. Olfactory cilia of the frog. *Journal of Cell Biology.* 25:209–230.

Restrepo, D., T. Miyamoto, B. P. Bryant, and J. H. Teeter. 1990. Odor stimuli trigger influx of calcium into olfactory neurons of the channel catfish (*Ictalurus punctatus*). *Science.* 249:1166–1168.

Revial, M. F., A. Duchamp, and A. Holley. 1978. Odour discrimination by frog olfactory receptors: a second study. *Chemical Senses and Flavour.* 3:7–21.

Schäfer, K., H. A. Braun, and C. Isenberg. 1986. Effect of menthol on cold receptor activity. *Journal of General Physiology.* 88:757–776.

Schäfer, K., H. A. Braun, and L. Kürten. 1988. Analysis of cold and warm receptor activity in vampire bats and mice. *Pflügers Archiv.* 412:188–194.

Schofield, P. R. 1988. Carrier-bound odorant delivery to olfactory receptors. *Trends in Neuroscience.* 11:471–472.

Sklar, P. M., R. R. H. Anholt, and S. H. Snyder. 1986. The odorant-sensitive adenylate cyclase of olfactory receptor cells. *Journal of Biological Chemistry.* 261:15538–15543.

Su, J. Y., and W. Hasselbach. 1984. Caffeine-induced calcium release from isolated sarcoplasmic reticulum of rabbit skeletal muscle. *Pflügers Archiv.* 400:14–21.